Microfluidics and Nanofluidics (2020) 24:24
https://doi.org/10.1007/s10404-020-2328-5

REVIEW

A concise review of microfluidic particle manipulation methods

Shuaizhong Zhang[1] · Ye Wang[1] · Patrick Onck[2] · Jaap den Toonder[1]

Received: 29 August 2019 / Accepted: 29 February 2020 / Published online: 19 March 2020

Abstract
Particle manipulation is often required in many applications such as bioanalysis, disease diagnostics, drug delivery and self-cleaning surfaces. The fast progress in micro- and nano-engineering has contributed to the rapid development of a variety of technologies to manipulate particles including more established methods based on microfluidics, as well as recently proposed innovative methods that still are in the initial phases of development, based on self-driven microbots and artificial cilia. Here, we review these techniques with respect to their operation principles and main applications. We summarize the shortcomings and give perspectives on the future development of particle manipulation techniques. Rather than offering an in-depth, detailed, and complete account of all the methods, this review aims to provide a broad but concise overview that helps to understand the overall progress and current status of the diverse particle manipulation methods. The two novel developments, self-driven microbots and artificial cilia-based manipulation, are highlighted in more detail.

Keywords Microfluidics · Particle manipulation · Self-driven microbots · Artificial cilia

1 Introduction

Controlled manipulation of particles (both synthetic and biological, e.g., cells) is desirable in both fundamental research and applications such as biomedical and biochemical research (Pamme 2007; Ateya et al. 2008; Nilsson et al. 2009; Xuan et al. 2010; Karimi et al. 2013), disease diagnostics and therapeutics (Gossett et al. 2010; Puri and Ganguly 2013), drug discovery and delivery systems (Dittrich and Manz 2006; Kang et al. 2008; Nguyen et al. 2013), and self-cleaning and antifouling technologies (Callow and Callow 2011; Kirschner and Brennan 2012; Nir and Reches 2016). For example, in bio-microfluidics, manipulation of a single particle or cell enables the revelation of subtle differences among individual cells not seen at population level. Microfluidics, where fluids are manipulated in microchannels (Whitesides 2006), is a promising technology to realize biomedical and biochemical devices for diagnostics and therapeutics, due to its unique advantages over conventional technologies including (i) reduced reagent consumption and thus low cost, (ii) high precision and throughput, (iii) flexible spatial and temporal control over fluid flow, (iv) in situ real-time observation, and last but not least (v) the possibility of diverse function integration by exploiting the full capability offered by microengineering (Whitesides 2006; Bhatia and Ingber 2014; Kim et al. 2019). To date, microfluidic technologies offer a wide range of possibilities for particle manipulation including transportation, separation, trapping, and enrichment, based on hydrodynamic, acoustic, electrical, optical and magnetic techniques (Laurell et al. 2007; Lenshof and Laurell 2010; Pratt et al. 2011; Sajeesh and Sen 2014; Lu et al. 2017; Ozcelik et al. 2018).

Recent advancement in micro- and nano-engineering offers us another tool to manipulate particles, namely through self-driven micro-robots in fuel solutions, such as hydrogen peroxide (Patra et al. 2013; Kim et al. 2018). This technique, which is still in its early stages of development, has been demonstrated to be able to capture, transport and release particles and cargo such as medicines, with the potential to realize these tasks on demand.

Another particle manipulation method which has been recently proposed, finds its inspiration in nature, where non-reciprocally beating cilia (slender microscopic hair-like protrusions of cells) act to transport fluids and particles in

✉ Jaap den Toonder
j.m.j.d.toonder@tue.nl

[1] Department of Mechanical Engineering and Institute for Complex Molecular Systems, Eindhoven University of Technology, 5600 MB Eindhoven, The Netherlands

[2] Zernike Institute for Advanced Materials, University of Groningen, 9747 AG Groningen, The Netherlands

many biological systems (Clifford 1932; Blake and Sleigh 1974; Enuka et al. 2012; den Toonder and Onck 2013a). Two specific examples are the transportation of egg cells to the uterus by motile cilia lining the inner walls of the fallopian tubes (Fauci and Dillon 2005; Enuka et al. 2012), and the transportation of mucus and infectious agents out of the respiratory tract by motile cilia in the mammalian lung and windpipe (Sleigh 1989; Enuka et al. 2012). Motivated by these examples, researchers have used simulations to study the capability of artificial cilia to manipulate fluids and particles and repel fouling agents from the ciliated surface (Khaderi et al. 2010, 2012; Masoud and Alexeev 2011; Semmler and Alexeev 2011; Dayal et al. 2012; Balazs et al. 2014; Tripathi et al. 2014). Recently, experimental works have shown the possibility to manipulate particles and water droplets using artificial cilia (Kim et al. 2015; Ben et al. 2018; Lin et al. 2018; Yang et al. 2018; Zhang et al. 2019).

This article aims to review and discuss the basic working principles of these particle manipulation methods, including a discussion of pros and cons of each method. The intended scope of the paper is to provide a broad but concise overview that helps to understand the overall progress and current status of the diverse particle manipulation methods, rather than offering an in-depth and detailed account of all the methods. Also, we do not claim to be complete in all the diverse aspects of the methods, but we provide the interested reader with references to more detailed review articles about particular methods. The two novel developments, self-driven microbots and artificial cilia-based manipulation, are highlighted in more detail. We first discuss particle handling in microfluidic systems, followed by cargo delivery with self-driven microbots. Then, we discuss particle manipulation examples by cilia in nature, which has inspired the numerical modelling work on artificial cilia to manipulate particles. Following these, we review the recent developments in experimental works on artificial cilia for particle manipulation. To conclude, we give a brief summary of these methods, as well as recommendations for future development of particle manipulation platforms.

2 Microfluidic methods for particle manipulation

2.1 Hydrodynamic methods

Hydrodynamic methods for particle manipulation utilize sophisticated microchannel networks to control particles primarily through balancing opposing transverse forces acting on the particles moving along a microfluidic channel. Detailed reviews of these methods can be found in Karimi et al. (2013) and Di Carlo et al. (2007). Examples of hydrodynamic forces are (1) the wall repulsion force (F_{wall}) originating from the asymmetry of the vorticity around the particles, pushing the particles away from the wall, and (2) the shear-gradient lift force (F_{shear}) originating from the curvature of the shear flow profile, which leads the particles to migrate away from the central axis (Karimi et al. 2013). Due to the competition between these two forces, particles suspended in the fluid migrate across streamlines when flowing downstream, and finally equilibrate at a specific location in the channel's cross section (Fig. 1a). The lateral equilibrium positions of the particles depend on the particle properties (size and deformability), channel size, flow rate and fluid properties (mass density and viscosity).

One representative hydrodynamic particle manipulation example is given by Bhagat et al. (2011). As shown in Fig. 1b, by designing the microfluidic device featured with two contraction–expansion regions, they successfully isolated rare cells from a whole blood sample with a throughput of ~ 10^8 cells/min and a collection efficiency of ~ 80%. The device works like this: in the first contraction–expansion region, all the cells equilibrate efficiently along the channel sidewalls under the influence of shear forces (Fig. 1b_X); in the second contraction–expansion region, the rare cells are aligned along the channel center by the pinching channel that is slightly smaller than the rare cells, while other cells remain close to the sidewalls because they are much smaller than the channel (Fig. 1b_Y); finally, rare cells are separated from the whole blood after a channel expansion (Fig. 1b_Z).

Amongst the studies using hydrodynamic methods to manipulate particles, the majority rely on fluidic inertial effects in addition to the wall repulsion force and the shear-gradient lift force. The generally used one is the so-called Dean flow that can occur in a channel with curved geometry. The formation of Dean flow in a curved channel can be summarized as follows (Bhagat et al. 2008; Karimi et al. 2013): due to inertial effects, the curvature of the channel induces two symmetric vortices in the top and bottom halves of the channel's cross section, leading to the formation of a pressure gradient in the radial direction (Fig. 1c). Particles present within the channel will experience a shear lift force, a wall repulsion force, as well as a Dean drag force, and thus they equilibrate at specific cross-sectional positions within the channel determined by the balance of these forces, which depends on the channel geometry, flow rate and particle size. By creating Dean flows in a serpentine channel, Di Carlo et al. (2007) succeeded in particle and cell-focusing with no discernable damage to cells (Fig. 1d). Much depending on cell type, cells may be damaged or affected by high shear rates—the circulating blood cells used by Di Carlo et al. (2007) were shown to remain viable up to a typical shear rate of 10^3 s^{-1}. However, their total channel network occupies a large surface area. In this regard, spiral-shaped channels

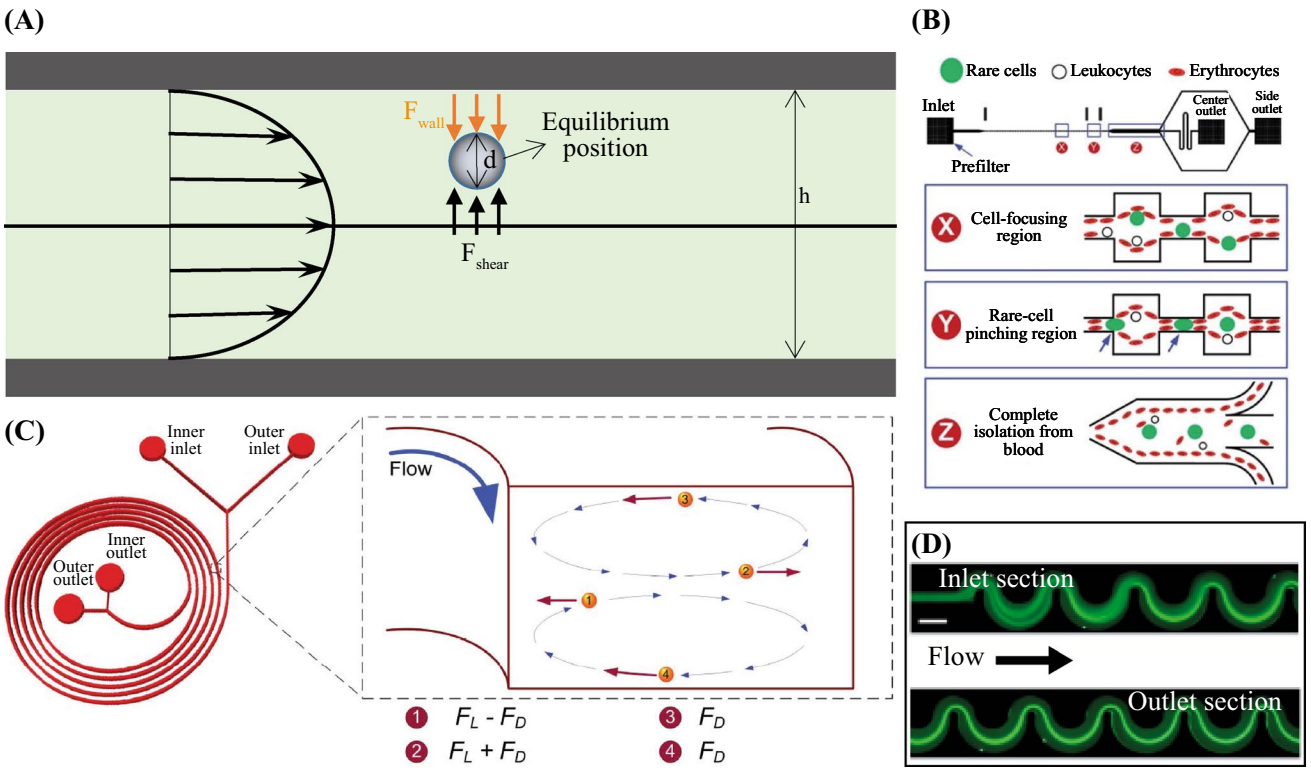

Fig. 1 Hydrodynamic particle manipulation methods. **a** Schematic illustration of the forces on a suspended particle and the equilibrium position of the particle in a fully developed flow in a confined channel. *d* is the size of the particle and *h* is the width of the channel. **b** Schematics of a rare cell-isolation microfluidic device. The microchannel consists of two large width–height ratio areas featured with contraction–expansion arrays for cell-focusing and rare cell-pinching (Bhagat et al. 2011). (Reprinted with permission, Copyright 2011, Royal Society of Chemistry). **c** Schematics of the Dean flow in a spiral microfluidic device: neutrally buoyant particles experience lift forces (F_L) and Dean Drag (F_D), which results in differential particle migration within the microchannel (Bhagat et al. 2008) (Reprinted with permission, Copyright 2008, Royal Society of Chemistry). **d** Fluorescent microscopy images of particle focusing in a serpentine channel (Di Carlo et al. 2007). The scale bar is 160 µm (Reprinted with permission, Copyright 2007, The National Academy of Sciences of the USA)

are often used as they yield a sufficiently long channel while occupying a relatively small surface area (Bhagat et al. 2008; Kuntaegowdanahalli et al. 2009).

Other hydrodynamic methods rely on the presence of micro-structures or micro-patterns in the channel to spatially redirect particles or cells of specific size or stiffness, for example posts, ridges and grooves, by introducing particular flow patterns. The approach that makes use of specifically designed arrays of micropillars within microchannels to sort particles based on their size is called "Deterministic Lateral Displacement" (DLD), first proposed by Huang et al. (2004). A difference with the methods discussed above is that DLD operates at low Reynolds numbers and does not rely on inertial effects. Recent reviews of DLD can be found in McGrath et al. (2014) and Salafi et al. (2019). Examples of approaches in which particle stiffness is utilized to sort the particles can be found in Wang et al. (2013) and Islam et al. (2017). Finally, adhesion-based sorting has been applied, in particular for cells, in which the target cells selectively bind to specific ligands or other functional coatings applied to the microfluidic channel walls, see, for example, Didar and Tabrizian (2010).

These techniques enable particle manipulation with high throughput and efficiency. However, they are mainly limited by the narrow range of working flow rate, and the strong dependence on channel structures and particle concentration. Moreover, the high shear rate in the inertial approaches may impact cell viability. Finally, some of the microfluidic devices, especially those with sophisticated channel structures and multiple constrictions at the outlets, are prone to clogging problems.

2.2 Acoustic method

The acoustic method for the manipulation of particles, termed acoustic tweezers, offers a non-contact mode of particle handling (reviewed by Laurell et al. 2007; Ozcelik et al. 2018). Figure 2a shows a typical standing-wave-based acoustic tweezer (Ozcelik et al. 2018), where the transducer converts electrical signals into acoustic waves.

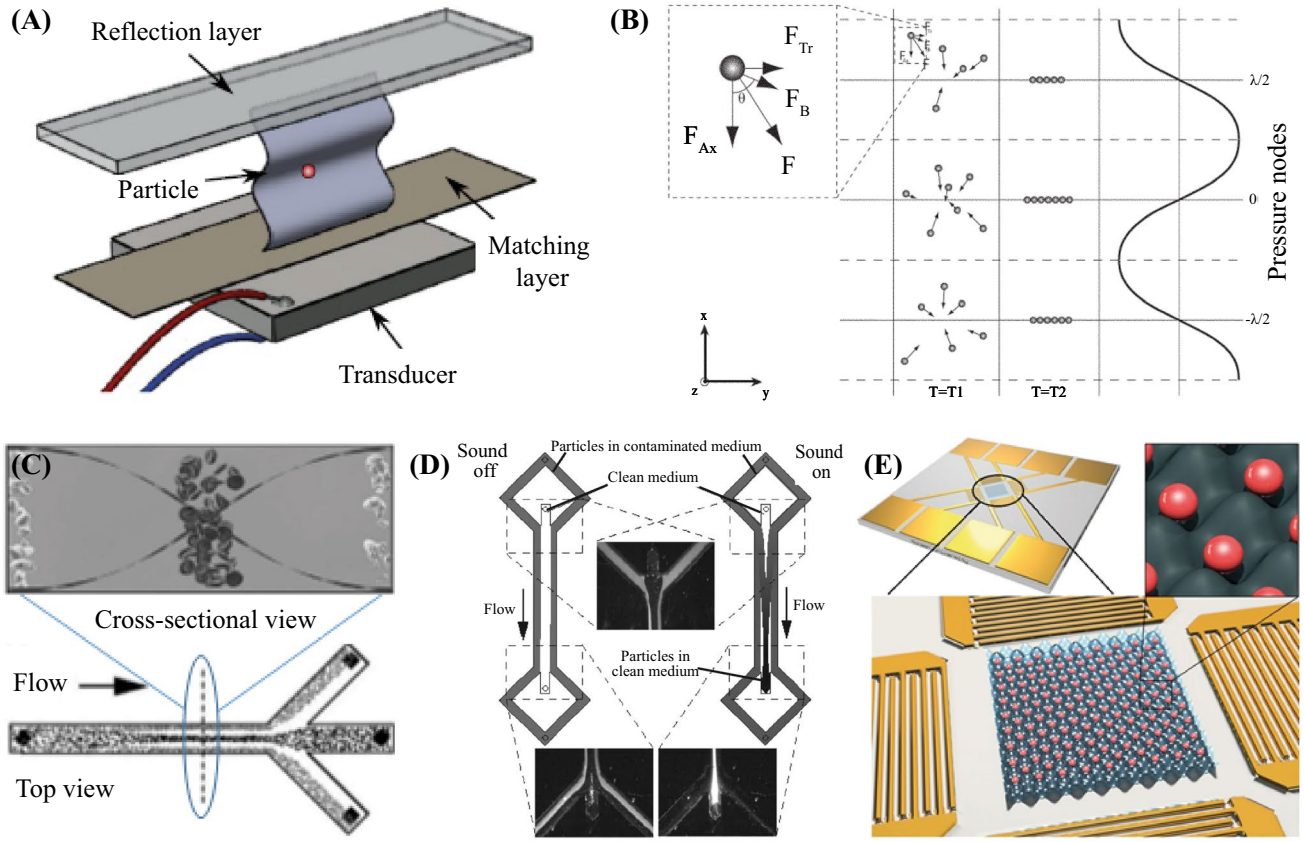

Fig. 2 Particle manipulation by acoustic methods. **a** A typical standing-wave-based acoustic tweezer. Acoustic waves reflected from the reflection layer form standing waves and establish a pressure distribution in the fluid. Through adjustment of the frequency with respect to the distance between the matching layer and the reflection layer, the number of pressure nodes and antinodes in the channel can be tailored (Ozcelik et al. 2018). (Reproduced with permission, Copyright 2018, Springer Nature America). **b** Schematics of particle manipulation using acoustic tweezers: F_{Ax} is the axial component of the acoustic radiation force, F_{Tr} is the transverse component and F_B is the interparticle force. At time T_1, the acoustic forces are initiated to act on the particles, and by time T_2, a steady state has been reached (Laurell et al. 2007). **c** Illustration of acoustically separating lipids (white) from red blood cells (black). The lipid particles are collected at side outlets, while the red blood cells are collected at the central outlet (Laurell et al. 2007). **d** Schematic illustration of an acoustic medium exchange/particle washing principle. In laminar flow conditions, the particles exit through the side outlets when the ultrasound is off, and they exit through the central outlet when the ultrasound is on (Laurell et al. 2007) (**b**–**d** are reprinted with permission from Laurell et al. 2007, Copyright 2007, Royal Society of Chemistry). **e** Schematic depiction of 2D single-cell patterning with one cell per acoustic pressure node using four interdigitated acoustic transducers (Collins et al. 2015) (Reprinted with permission, Copyright 2015, Macmillan Publishers Limited: Nature Communication)

The interference between waves reflected back and forth by the reflection and matching layer form standing waves and establish a pressure distribution in the fluid. The fundamental theory on particle manipulation utilizing acoustic tweezers shows that particles tend to gather at either the pressure nodes or the antinodes of the acoustic wave, under the impact of acoustic radiation forces acting on the particle, as shown in Fig. 2b (Laurell et al. 2007). Generally, solid particles and most cells gather at the pressure nodes; while, air bubbles and lipid vesicles are focused at the antinodes. The contact-free mode of acoustic tweezers makes this method interesting for manipulating vulnerable particles, e.g., cells. In principle, the acoustic method can be applied to all types of suspended particles that have acoustic properties that differ from those of the surrounding medium (i.e., the liquid in which the particles are suspended) (Laurell et al. 2007). Acoustic tweezers form a versatile tool for particle manipulation because of their favorable properties including (i) the ability to manipulate both fluids and particles, (ii) the ability to manipulate particles in a variety of different media (for example, air, aqueous solutions, undiluted blood, and sputum); (iii) the ability to manipulate particles, cells, and organisms across a wide range of length scales, from nanometers (for example, exosomes and nanowires) to millimeters (for example, C. elegans); (iv) the ability to select and to manipulate a single particle or a large group of particles (for example, billions of cells); and (v) the

ability to handle fluidic throughputs ranging from 1 nL/min to 100 mL/min (Ozcelik et al. 2018). Representative applications of particle manipulation by acoustic standing waves are: (1) continuous particle separation in a streaming channel with multiple outlets based on that particles with different acoustic properties have different equilibrium positions within ultrasonic standing waves, for example, red blood cells tend to gather at the pressure nodes while lipids move away from the pressure nodes, as exemplified in Fig. 2c (Petersson et al. 2004); (2) medium exchange or particle washing by laminating different media and manipulating the position of particles with respect to different media layers under laminar flow conditions, (Fig. 2d) (Hawkes et al. 2004; Petersson et al. 2005); and (3) particle patterning (Fig. 2e) (Collins et al. 2015). Finally, acoustic holograms can be created using discrete and independently driven ultrasound sources, or by combining a patterned acoustic lens with a single transducer, to controllably and simultaneously manipulate multiple particles along specific paths in a fluid (Melde et al. 2016).

Nonetheless, there are also limitations of acoustic particle manipulation. For example, the design and fabrication of acoustic systems is a tedious and complex task, rendering the acoustic systems to be costly. Moreover, it is only efficient for suspended particles, and even though the principle is suitable for a wide range of particle sizes and flow rates, the effect is quite dependent on the specific device design and therefore, specific device configurations can only be designed for a narrow range of particle concentration and size, as well as flow rate.

2.3 Electrical methods

Particles can be manipulated in microfluidic device using electrical fields in various ways. We will briefly discuss here electrophoresis, electro-osmosis, and dielectrophoresis. An in-depth review of these is given by Xuan (2019).

Electrophoresis (EP) is the movement of an electrically charged surface relative to a stationary liquid, induced by an applied electric field. This effect can be used to transport, sort, or trap charged particles within a liquid. It only works if the conductivity of the liquid is relatively low, implying a low presence of ions that otherwise would accumulate around the charged particle and (partly) neutralize its charge, an effect known as electrical screening. This poses limitations to the application of EP, both on the particles and on the fluid. A major application that uses the mechanism is that of electrophoretic displays (i.e., electronic paper), that contain microfluidic pixels in which oppositely charged particles with different optical properties are transported and trapped to switch the pixel, see Fig. 3A.

Electro-osmosis (EO) is the movement of a liquid relative to a charged (AC electro-osmosis, ACEO) or polarizable (Induced-Charge Electro-osmosis, ICEO) surface (for example of a microchannel) induced by an electric field. In both ACEO and ICEO, an electrical double layer (EDL) is established at the liquid–solid interface. The counter-ions in the liquid phase of the EDL can be set into motion by applying an electric field parallel to the wall. The mobile ions drag bulk liquid in the direction of the electric force. ACEO can generate strong liquid flow when using well-designed electrode patterns on the surface (Huang et al. 2010), and this flow can be used to manipulate particles (Xuan 2019). Wu

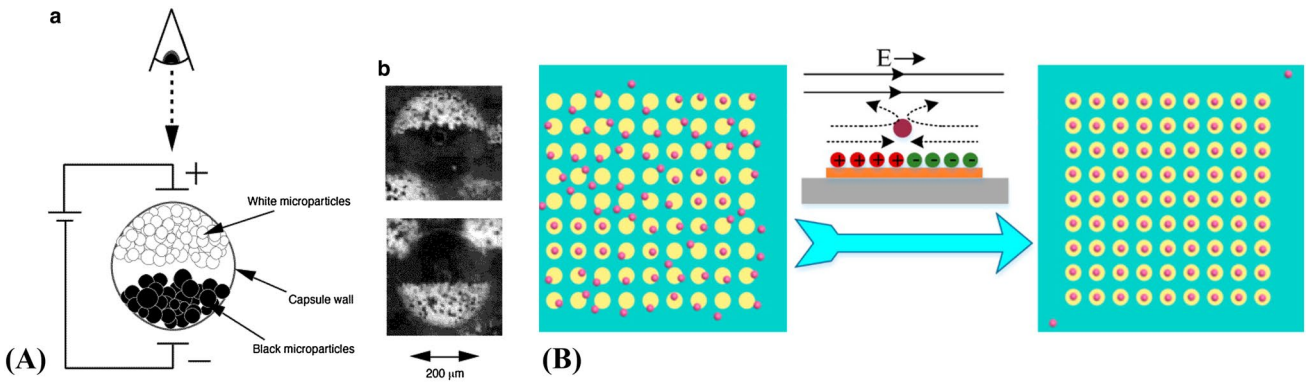

Fig. 3 Particle manipulation by electrophoresis and electro-osmosis. **A** (a) Schematic illustration of microencapsulated electrophoretic image display (white and black microparticles system). The top transparent electrode becomes positively charged, resulting in negatively charged white microparticles migrating towards it. Oppositely charged black microparticles move towards the bottom electrode. (b) Photomicrograph of an individual microcapsule addressed with a positive and negative field (Comiskey et al. 1998). (Reprinted with permission, Copyright 1998, Nature, Macmillan Publishers Ltd). **B** Induced-charge electro-osmosis (ICEO) can be used to trap particles on arrays of floating electrodes: initially randomly distributed particles are focused to the center of the floating electrodes and immobilized by the interaction between ICEO flow and gravitational force (Wu et al. 2016) (Reprinted with permission, Copyright 2016, American Chemical Society)

et al. (2016) have shown that ICEO in combination with a rotating electrical field can be used to trap cells and particles on an electrode array when the electrodes are well designed, as illustrated in Fig. 3B.

Dielectrophoresis (DEP) was first investigated by Herbert Pohl in the 1950s (Pohl 1951). In DEP, a non-charged dielectric particle is subjected to a dielectric force in a non-uniform (often Alternating Current) electric field. The strength of the force depends on the dielectric properties of both the surrounding medium and the particle, on particle shape and size, and on the frequency of the applied electric field (Lenshof and Laurell 2010). This force moves the particle towards or away from the stronger electric field (Fig. 4a) (Lenshof and Laurell 2010): (i) when particles have higher permittivity than the surrounding fluid they are pushed towards the stronger electric field, and this is called positive dielectrophoresis (pDEP); (ii) when having lower permittivity than the fluid the particles are repelled from the higher electric field, which is consequently called negative dielectrophoresis (nDEP). Dielectrophoresis is extensively used for particle/cell trapping (Cummings and Singh 2003; Gadish and Voldman 2006), separation (Fig. 4b) (Adams et al. 2008) and exchange or washing (Fig. 4c) (Tornay et al. 2008). Advantages of dielectrophoresis are that it works for non-charged particles as long as they are polarizable, and that it offers flexibility in setting particle sorting thresholds (e.g., particle size) simply by adjusting the electric field frequency. However, this technology is highly dependent on particle or

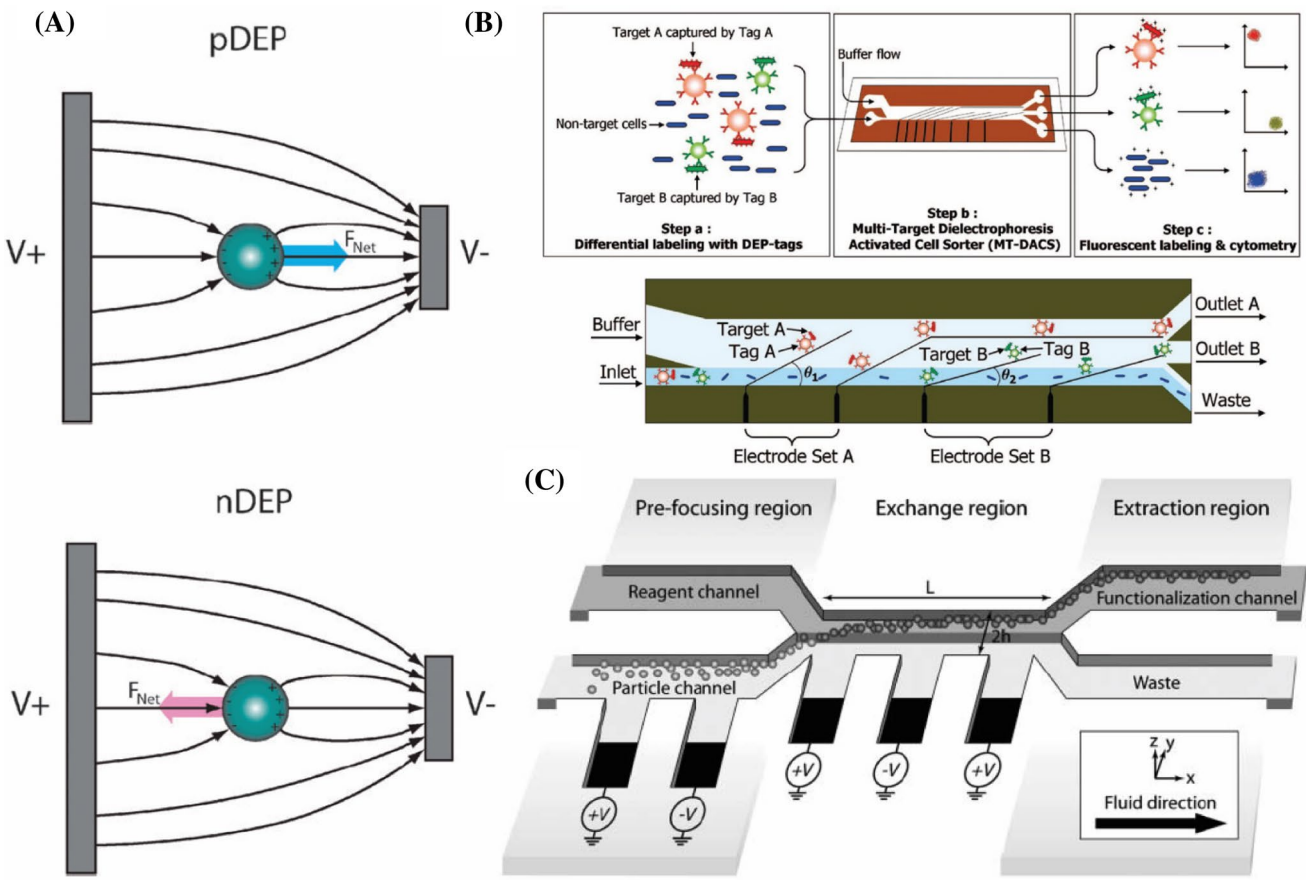

Fig. 4 Particle manipulation by dielectrophoresis. **a** Schematics of the dielectric force on a dielectric particle in both positive dielectrophoresis (pDEP) and negative dielectrophoresis (nDEP) (Lenshof and Laurell 2010). (Reprinted with permission, Copyright 2010, Royal Society of Chemistry) **b** Schematics of multi-target cell sorting procedure using DEP with two sets of electrodes that are positioned at different glancing angles. Target A cells labeled with tag A are separated at electrode set A and exit through outlet A. Target B cells labeled with tag B are selected at electrode set B and exit through outlet B. The unlabeled, non-target cells are not deflected by either electrode set, and they exit through the waste outlet. Target B cells are not selected at electrode set A because the dielectric force applied on them is too low to counter the hydrodynamic force by the flow (Adams et al. 2008). (Reprinted with permission, Copyright 2008, American Chemical Society). **c** Particle exchanger using DEP in a microfluidic channel network featured with three functional regions: (i) the pre-focusing region, where particles are pushed close to the inner wall of the particle channel to reduce the exchanging distance in (ii) the exchange region, where the particles are pushed into the reagent and exit in (iii) the extraction region, where the two liquids are split again (Tornay et al. 2008) (Reprinted with permission, Copyright 2008, Royal Society of Chemistry)

cell polarizability and generally requires low-conductivity media, which limits its use in cell related applications.

An interesting extension of DEP-based particle manipulation has lead to "optoelectronic tweezers" (OET) (Wu 2011). An OET device contains a photosensitive layer of which the electrical conductivity can be sensitively controlled by illumination. Hence, local illumination by a light beam allows to switch on an off 'virtual electrodes' in desired patterns, creating electrical field gradients inside microfluidic devices that can be used to perform DEP-based particle manipulation. OET combines the advantages of two particle manipulation techniques: electrode-based DEP and optical tweezers (see the next section). An advantage of OET is its elegance in electrical field control, without the need for complex electrode patterns, and the method does not require high optical intensities like optical tweezers do.

2.4 Optical tweezers

Optical tweezers were pioneered by Ashkin et al. (1986). They comprise the use of a tightly focused laser beam to trap and manipulate particles or cells with very high precision (see the review by Lenshof and Laurell 2010). The basic mechanism is as follows: the laser beam with a Gaussian intensity profile carries momentum that is partially transferred to the particle/cell when the beam hits the object, and this generates a net force on the object towards the center of the beam; thus, the object is trapped by the beam and follows the motion of the beam (Molloy and Padgett 2002; Dholakia et al. 2008; Lenshof and Laurell 2010). Figure 5a shows an example of high-precision molecule manipulation with dual-beam optical tweezers where molecular knots were successfully tied in nano-filaments of actin (Arai et al. 1999). Another example of particle manipulation using optical tweezers is given by MacDonald et al. (2003) where a three-dimensional optical lattice selectively deflects one species of particle into the upper flow field, creating particle-size-based fractionation (Fig. 5b). By using a liquid–crystal spatial light modulator, a time-dependent hologram can be generated that produces a dynamic optical landscape with multiple traps, so that multiple particles can be independently transported along complex trajectories (Grier and Roichman 2006). Despite being a powerful tool for force spectroscopy and biomolecular manipulation, traditional optical tweezers require complex optics, including high-powered lasers and high-numerical aperture objectives, and they are potentially damaging to biological samples.

2.5 Magnetic methods

With magnetic methods, use is made of a magnetic field generated either by a permanent magnet or by electromagnets to manipulate particles, see the detailed reviews of Van Reenen et al. 2014 and Puri and Ganguly 2013. In a non-uniform magnetic field, a magnetic or magnetically labelled particle/cell is attracted towards the higher magnetic field. The magnetic force depends on the magnetic field gradient and also on the size and magnetic properties of the particle/cell. One typical application is the continuous particle separation based on particle size as particles with the largest magnetic volume experience the strongest magnetic forces and consequently end up in an outlet closer to the magnet (Fig. 6A) (Pamme and Manz 2004). However, the spatial resolution of this technique is relatively low and it requires a strong magnetic field gradient and therefore the working distance is limited.

Being able to manipulate magnetic particles also enables microfluidic mixing (Van Reenen et al. 2014) which

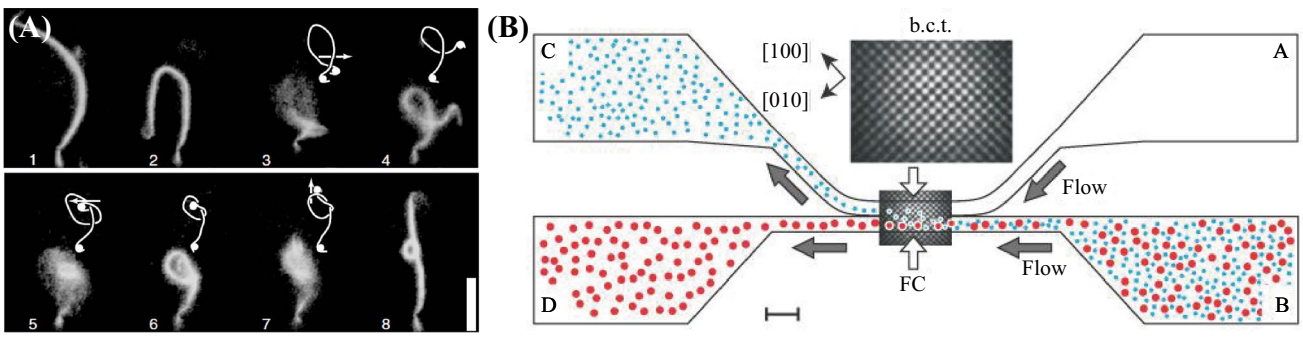

Fig. 5 Particle manipulation by optical tweezers. **a** Knotting an actin nanofilament using a dual-beam optical tweezers. To each end of the filament, a myosin-coated polystyrene bead is attached that can be manipulated by the optical tweezers. While keeping one optical trap fixed, the other one moves the polystyrene bead so as to tie a knot on the filament. The scale bar is 10 μm (Arai et al. 1999). (Reprinted with permission, Copyright 1999, Macmillan Publishers Ltd: Nature). **b** Particle sorting based on particle size and optical properties using a three-dimensional optical lattice—a body-centered tetragonal (b.c.t.) lattice in a fractionation chamber (FC). The array of laser beams deflects one species of particles towards the center of a laser beam iteratively, and finally pushes these particles into the upper fluid stream. Scale bar, 40 μm (MacDonald et al. 2003) (Reprinted by permission from MacDonald et al. (2003), Copyright 2003, Nature Publishing Group)

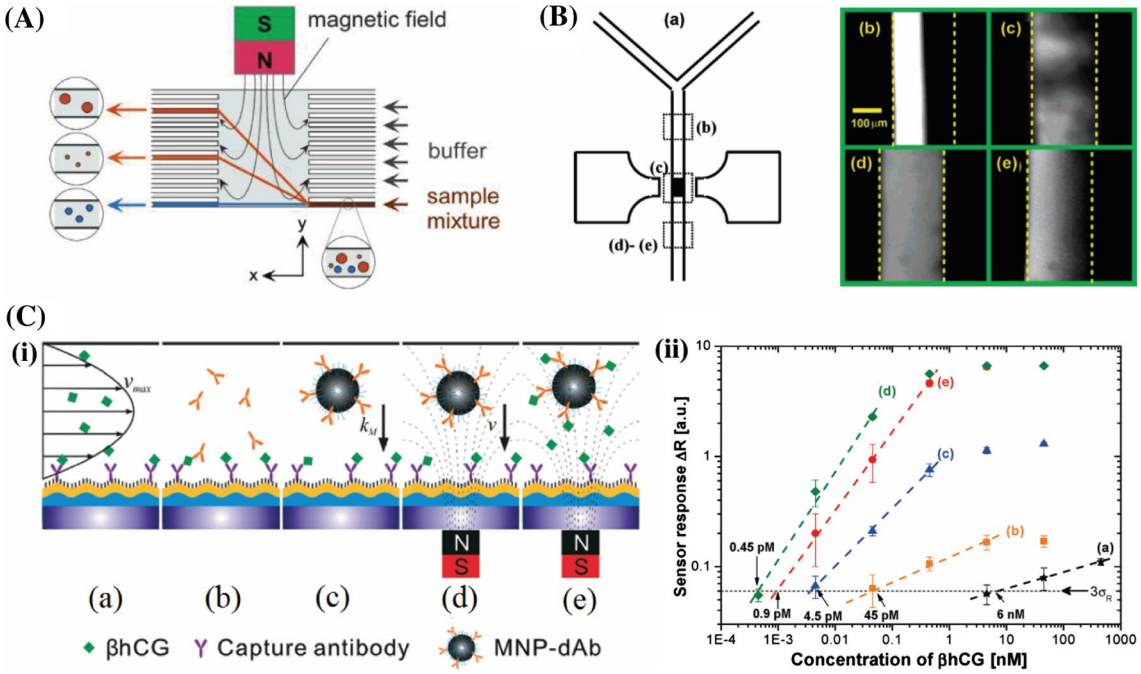

Fig. 6 Particle manipulation with magnetic methods. **A** Magnetophoresis according to Pamme et al. A sample suspension is pumped into a separation chamber where a non-uniform magnetic field is applied perpendicular to the direction of the flow. Magnetic particles (red) will be attracted to the higher magnetic field according to their size and magnetic susceptibility and are, thus, separated from each other and from nonmagnetic material (blue) (Pamme and Manz 2004). (Reprinted with permission, Copyright 2004, American Chemical Society). **B** Microfluidic mixing with magnetically retained and actuated magnetic particles. (a) Schematic diagram of the microfluidic design. The fluorescence images (b–e) on the right are taken at different locations as indicated in panel (a), i.e.: (b) before mixing; (c) during mixing; (d) after mixing by a 20 Hz sinusoidal field; and (e) after mixing by a 5 Hz square-shaped field (Rida and Gijs 2004). (Reprinted with permission, Copyright 2004 American Chemical Society). **C** Magnetic nanoparticle-enhanced biosensor based on grating-coupled surface Plasmon resonance (SPR) for detecting β human chorionic gonadotropin (βhCG). (i) Schematics of used detection formats: direct detection (a), sandwich assays with amplification by detection antibody (b) and magnetic nanoparticles coated with detection antibodies (MNP-dAb) without (c) and with (d) applied magnetic field. (e) Detection format consisting of preincubating MNP-dAb with βhCG followed by sandwich assay upon applied magnetic field gradient. (ii) The dose–response curves for the detection of βhCG by direct detection format (a, stars), followed by antibody amplification (b, squares) and the amplification by MNP-dAb without (c, triangles) and with (d, diamonds) an external magnetic field. In format e, a sample with βhCG was incubated with MNP-dAb, followed by the detection of the MNP-dAb-βhCG complexes with external magnetic field applied (circles) (Wang et al. 2011) (Reprinted with permission, Copyright 2011 American Chemical Society) (color figure online)

is an essential step for biochemistry analysis, drug delivery and sequencing or synthesis of nucleic acids (Nguyen and Wu 2005). One representative example is shown in Fig. 6B, where two parallel streams are mixed (95% mixing efficiency) within a mixing length of only 400 µm at a flow velocity on the order of 0.5 cm/s (Rida and Gijs 2004). The efficient fluid mixing was attributed to the chaotic splitting of fluid streams through the dynamic and randomly porous structure of the particle aggregate and the relative motion of the fluid with respect to the magnetic particles. Fundamental advances in the development of magnetic particles have been driving the increasing popularity of the magnetic method. To date, biofunctionalized magnetic particles with, e.g., antibodies have been used for capture and detection of analytes (Van Reenen et al. 2014), for drug discovery, as well as to provide personalized therapy (Puri and Ganguly 2013). As shown in Fig. 6C, magnetic manipulation of magnetic nanoparticles coated with detection antibodies clearly had a positive effect on the obtained dose–response curve, and led to detection limits within the picomolar range (Wang et al. 2011). However, it is necessary to pretreat the magnetic particles, such as coating with antibodies, so as to perform a specific task, and these functionalized magnetic particles have limited applications since the coated labels only respond to specific targets.

The shape of the magnetic particles can be tuned to enhance the controllability of the particle manipulation. For example, helical magnetic microstructures have been developed with controllable transportation direction induced by a rotating magnetic field (Tottori et al. 2012). Also, collective behavior of magnetic microparticles can be exploited to induce swarm-like behavior with control over transportation and navigation in fluids (Yu et al. 2019).

3 Self-driven microbots as particle transporters

Advances in micro/nanotechnologies have made it possible to fabricate self-driven micro/nano-robots to transport and release particles/cargos on demand for various applications including drug delivery and biochemical sensing (for more detailed reviews, see Patra et al. 2013 and Kim et al. 2018). Micro/nano-robots are often bio-inspired, such as hybrid bio-synthetic nanomotors that incorporate motor proteins [e.g., kinesin (Block and Schnitzer 1997), myosin (Kitamura et al. 2005), RNA polymerase (Block et al. 1998), F_1—adenosine triphosphate synthase (Soong et al. 2000)] or living organisms [Mycoplasma mobile bacteria (Hiratsuka et al. 2006), flagellated cells (Darnton et al. 2004; Magdanz et al. 2013)] into synthetic systems. Towards real-life applications, particle manipulation in a more controlled manner is in high favor for, e.g., targeted drug delivery. In this regard, catalytic reaction-powered microbots, moving in fuel solutions such as hydrogen peroxide, have been intensively studied (Patra et al. 2013; Kim et al. 2018). The predominant driving force originates from bubbles generated during the catalytic reaction. One representative case is the Au–Pt bimetallic nanorod devised by Sen et al. (Fig. 7A) (Paxton et al. 2004), where the two ends of the nanorod were coated with gold and platinum, respectively. The method is based on the feature that platinum is an active hydrogen peroxide decomposition catalyst while gold is not. Thus, oxygen is generated only at the Pt end, which creates a proton gradient along the axis of the rod from the Pt to Au, and this drives the nanorod at a speed of up to 20 μm/s with the platinum end facing forward. This nanomotor was demonstrated to be capable of transporting (Sen et al. 2008) and releasing colloidal cargos (Sundararajan et al. 2010). Wang et al. improved this design by introducing magnetic carbon nanotube (Au/Ni/Au/PtCNT) nanoshuttles (Fig. 7b) which had the ability to pick-up, transport and release magnetic cargo (Kagan et al. 2010). However, the efficiency of successful cargo pick-up relies strongly on the subtle magnetic attraction between the nanomotor and the cargo. Moreover, the cargo release extremely depends on the competition of the magnetic attraction and the shear drag force imposed on the cargo originating from the fast reversal in the direction of the nanomotor, which is very difficult to control.

Microtubular jet engines fabricated by rolling-up polymer films are another type of self-propelled micro/nano-robots (Mei et al. 2011). Schmidt and coworkers are the pioneers of this approach, and they fabricated the first version of the rolled up microtube which consists of (i) a catalyst layer, usually Pt, (ii) a magnetic layer, Fe, for magnetic manipulation, and (iii) a Ti/Au layer for good adhesion between layers (Fig. 8a) (Solovev et al. 2009). When immersed in aqueous hydrogen peroxide solutions, the microjet engines continuously generate oxygen microbubbles inside the cavity of the tubes that are released from one opening. Aided by a magnetic field acting on the Fe layer, this results in directional propulsion of the microjet engines at a speed of up to ≈2 mm/s (approximately 50 body lengths per second). Moreover, cargo loading and drop-off were demonstrated by such microtubular engines through catalytic reaction-induced inward flow and a rapid turning of the magnetic field, respectively (Fig. 8b) (Solovev et al. 2010). Wang's group is another pioneer of microtubular motors; they fabricated bilayer polyaniline (PANI)/platinum microtubes using an electrochemical growth method within conically shaped pores of a polycarbonate template membrane (Fig. 9A, B) (Gao et al. 2011). These mass-produced microjets are self-propelled at an ultrafast speed (> 350 body lengths per second), and can operate in very low fuel levels (down to 0.2% hydrogen peroxide). Such type of microjets was later on demonstrated to be capable of bacterial isolation by functionalizing the microjets with Concanavalin A lectin

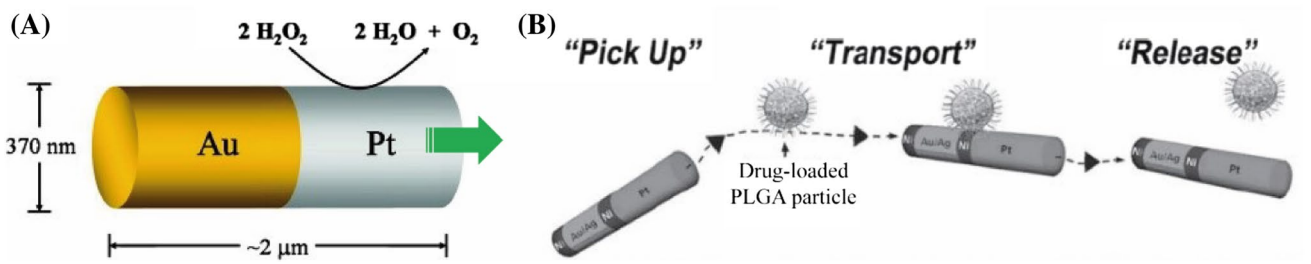

Fig. 7 **a** Schematic illustration of the self-propulsion mechanism of a Pt–Au nanomotor moving to the right with Pt end facing forward (Paxton et al. 2004) (Reprinted with permission, Copyright 2004, American Chemical Society). **b** Scheme of Au/Ni/Au/Pt nanoshuttles for cargo pick-up (via weak magnetic attraction between the nanoshuttle's magnetic nickel segment and the magnetic cargos), transport (through thrusts powered by catalytic reaction-generated bubbles) and release (attributed to the hydrodynamic drag forces imposed on the cargos) (Kagan et al. 2010) (Reprinted with permission, Copyright 2010, Wiley-VCH Verlag GmbH & Co. KGaA, Weinheim)

bioreceptors (Fig. 9C) (Campuzano et al. 2012). Wang et al. advanced this concept further by developing a polyaniline/Zn microrocket which self-propelled at a speed of 100 body lengths/s in strong acidic media by continuous generation of hydrogen bubbles at the inner zinc layer (Fig. 10A) (Gao et al. 2012). Such acid-powered microrockets were used

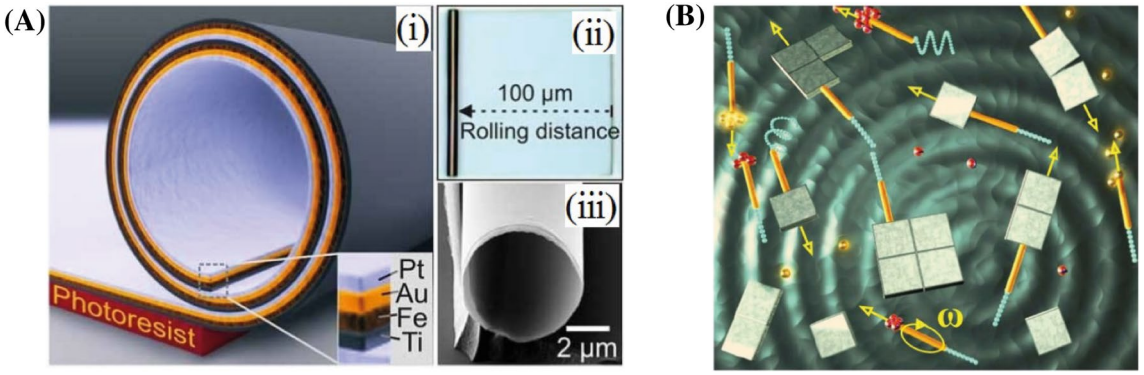

Fig. 8 **a** (i) Schematics of a rolled up microtube consisting of Pt/Au/Fe/Ti multilayers on a photoresist sacrificial layer. (ii) Optical microscopy and (iii) SEM images of a rolled up Pt/Au/Fe/Ti microtube (Solovev et al. 2009). (Reprinted with permission, Copyright 2009, Wiley-VCH Verlag GmbH & Co. KGaA, Weinheim) **b** Schematics of rolled up microtubes (golden) for loading, transporting, delivery and assembly of microparticles and nanoplates in fuel solution under wireless control by a magnet (Solovev et al. 2010) (Reprinted with permission, Copyright 2010, Wiley-VCH Verlag GmbH & Co. KGaA, Weinheim)

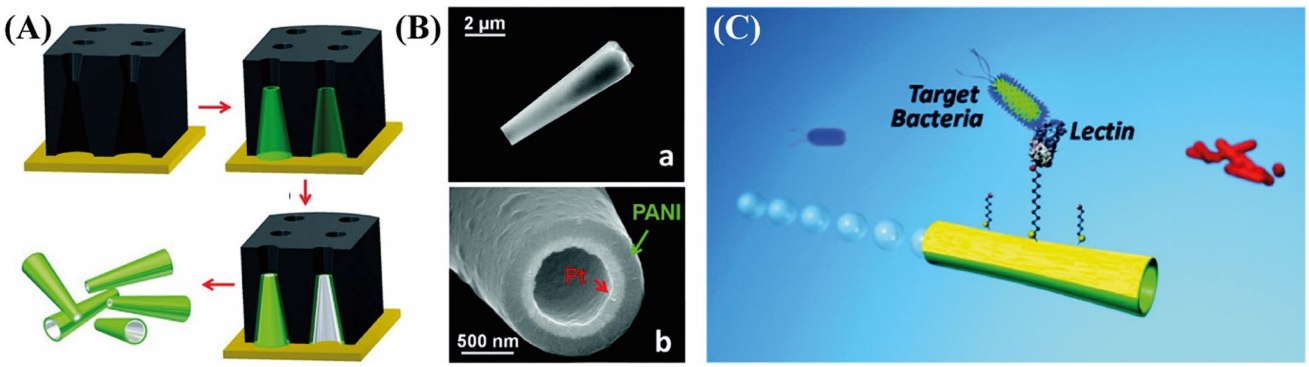

Fig. 9 **A** Schematics of fabrication of bilayer polyaniline (PANI)/Pt microjets using a cone-shaped polycarbonate template. **B** SEM images of the fabricated microjets: (a) side view and (b) cross view (Gao et al. 2011). (Reprinted with permission, Copyright 2010, Wiley-VCH Verlag GmbH & Co. KGaA, Weinheim). **C** Schematics of a lectin functionalized microjet for targeted bacterial capture and transport in hydrogen peroxide (Campuzano et al. 2012) (Reprinted with permission, Copyright 2011, American Chemical Society)

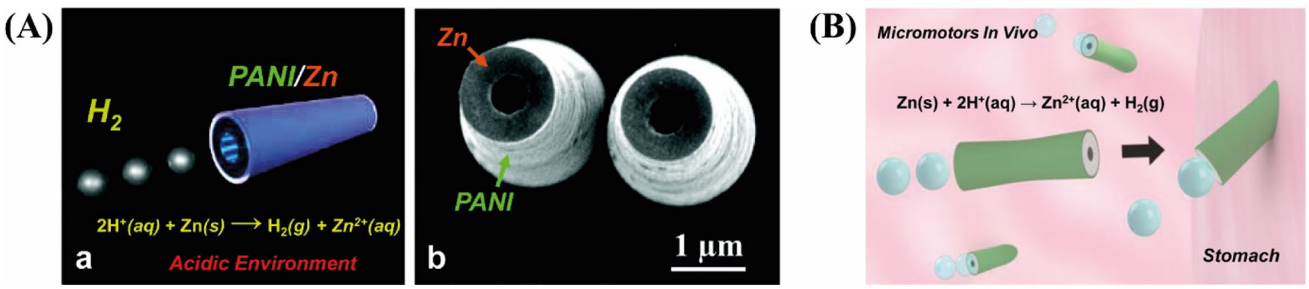

Fig. 10 **A** Schematic of acid-driven PANI–Zn microrocket: motion in an acidic environment (a); SEM images of the top view of two PANI–Zn microrockets (b) (Gao et al. 2012) (Reprinted with permission, Copyright 2011, American Chemical Society). **B** Schematic of the in vivo propulsion and tissue penetration of the zinc-based microrockets in a mouse stomach (Gao et al. 2015) (Reprinted with permission, Copyright 2014, American Chemical Society)

for cargo payloads delivery and drop-off in a live mouse stomach, which is one of the pioneering works demonstrating in vivo applications of microbots (Fig. 10B) (Gao et al. 2015).

Even though substantial progress has been made by micro/nano-robots in in vitro and in vivo studies, the research on micro/nano-robots is still in an early stage. Convincing proof-of-principle concepts have been demonstrated but the particle manipulation process is still time consuming and difficult to control. In addition, several specific challenges still need to be addressed for real-life applications. One fundamental challenge is the biocompatibility of the micro/nano-robot for in vivo applications. Another one is the fuel source for the self-driven robots, which for the moment are limited to hydrogen peroxide or strong acids, while they should be extended to organic molecules such as glucose present in living systems.

4 Particle manipulation by artificial cilia

Nature, after millions of years' evolution, offers us a rich source of inspiration to solve engineering and scientific problems. One nature-inspired method to manipulate particles is the use of artificial cilia—a general review of artificial cilia in microfluidic applications is given in den Toonder and Onck (2013a, b). Biological cilia are slender microscopic hair-like protrusions of cells with a typical length between 2 and 15 μm, which were first reported by Antony van Leeuwenhoek in 1675 (Clifford 1932), and have been found to exist ubiquitously in nature (den Toonder and Onck 2013a). This organelle has evolved to possess versatile functionalities including sensing (Blake and Sleigh 1974), pumping (Blake and Sleigh 1974), particle manipulation such as cell and food transportation and antifouling (Sleigh 1989; Fauci and Dillon 2005; Enuka et al. 2012; Strathmann et al. 1972; LaBarbera 1981, 1984; Taghon 1982; Fritz et al. 1984; Stafford-Smith and Ormond 1992; Wahl et al. 1998; Riisgard and Larsen 2001; Ruppert et al. 2004; Romero et al. 2010). Specific examples are (1) active cilia covering the outer surfaces of mollusks and coral can generate local currents, shielding away sand and preventing settlement of a wide variety of marine fouling organisms (Stafford-Smith and Ormond 1992; Wahl et al. 1998; Ruppert et al. 2004); (2) motile cilia line the windpipe and the lungs of the human body, helping to clean up mucus and dust out of the respiratory tract (Sleigh 1989; Enuka et al. 2012); (3) motile cilia line the inner walls of the fallopian tubes, transporting egg cells to the uterus (Fauci and Dillon 2005; Enuka et al. 2012); (4) cilia grow in the mouth of some marine suspension microorganisms, facilitating feeding (Strathmann et al. 1972; Riisgard and Larsen 2001; Romero et al. 2010). All of these favorable functionalities are dominated by the substantial local flow generated by the asymmetric motion of cilia in combination with the direct contacting forces applied on the particles by cilia beating.

Inspired by the impressive versatility of biological cilia in manipulating surrounding particulates and generating fluid flows, researchers have mimicked the biological function of natural cilia to create self-cleaning and antifouling surfaces. Via computational and theoretical models, the group of Balazs and co-workers have laid a foundation for future research on particle manipulation by cilia (Masoud and Alexeev 2011; Semmler and Alexeev 2011; Dayal et al. 2012; Balazs et al. 2014; Tripathi et al. 2014). Firstly, by performing a tilted conical motion, active adhesive cilia were proven to be able to regulate the motion of both rigid and soft microscopic particles (Fig. 11a, b) (Bhattacharya et al. 2012; Bhattacharya and Balazs 2013): (1) trapping particulates when the cilia–particle adhesion strength is relatively high, (2) propelling particulates at intermediate cilia–particle adhesion strength, (3) repelling or releasing particulates when the cilia–particle adhesion strength is relatively low. Secondly, active cilia were found to be effective in separating microscopic particles by both stiffness (because the traveling speed of rigid and compliant particles are different at both lower and higher cilia–particle adhesion) (Bhattacharya and Balazs 2013) and size (due to a higher critical adhesion strength required to capture larger particles, Fig. 11c) (Tripathi et al. 2013). Moreover, active cilia can also be used to drive away model swimming micro-organisms primarily due to their ability to generate powerful local flow (Fig. 11d) (Shum et al. 2013). Moreover, passive (rather than active) cilia were also demonstrated to be capable of repelling sticky particles away from the ciliated surface when the cilia are driven to undulate by an oscillatory shear flow (Fig. 11e) (Tripathi et al. 2014). All of these indicate the possibility to harness artificial cilia to manipulate particles and to create self-cleaning/antifouling surfaces.

Inspired by these fascinating modelling findings and insights, Zhang et al. (2018) fabricated magnetic artificial cilia (MAC) made of a polydimethylsiloxane (PDMS)—superparamagnetic particle (carbonyl iron powder, CIP) composite material. These MAC were demonstrated to be capable of generating versatile water flows in a microfluidic channel network by performing a tilted conical motion under the actuation of a rotating magnet, mimicking the motion of embryonic nodal cilia (Nonaka et al. 2005; Yoshiba et al. 2012; Zhang et al. 2018). The reason why this type of asymmetric motion can effectively induce fluid flows is that one cilium carries a larger volume of liquid when it beats more straight (effective stroke) than when it passes near the substrate (recovery stroke), thus generating a net flow in the same direction as the effective stroke in a complete beating cycle (Zhang et al. 2018). Subsequently, these MAC were employed to create self-cleaning

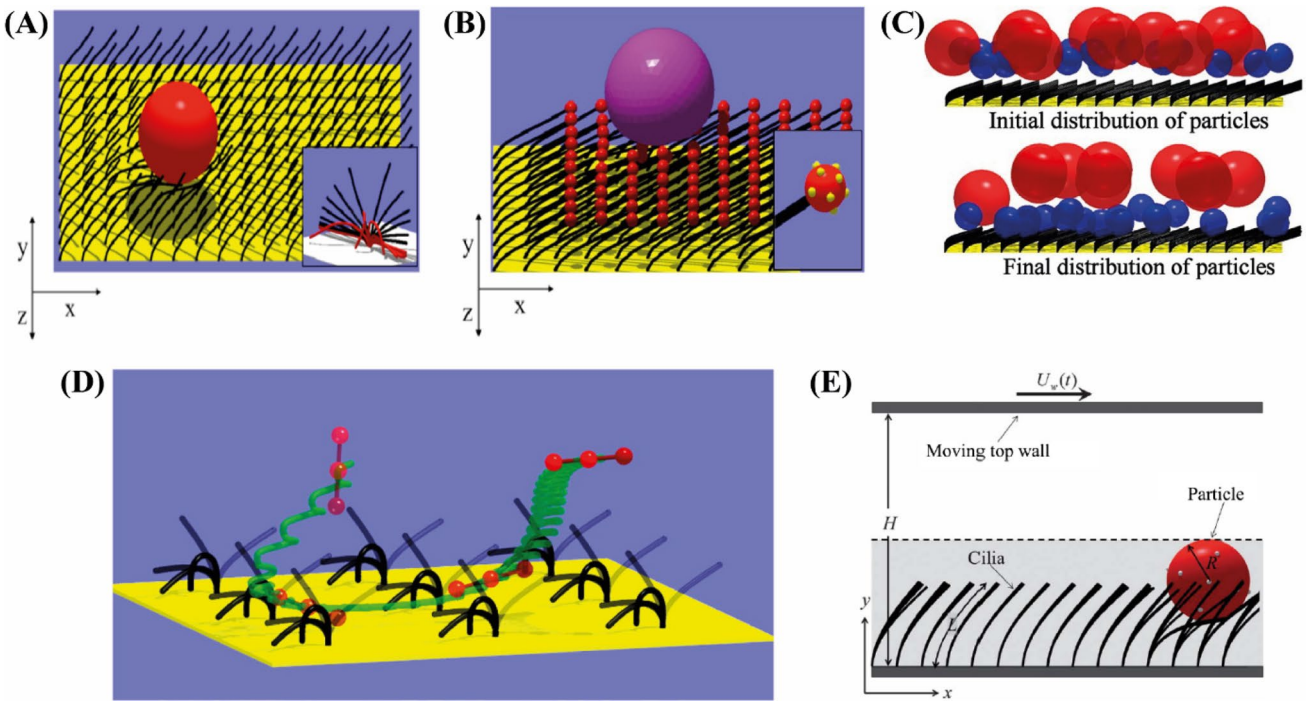

Fig. 11 Simulation works on particle manipulation by artificial cilia. **a** Cilia (black filaments) repel a rigid particle (the red sphere). The inset shows superimposed 3D motion of a cilium taken at equal time intervals during one beating cycle. The cilium is moving counter-clockwise. It is colored black when the tip moves in the negative x direction (effective stroke) and red when the tip moves in the positive x direction (recovery stroke) (Balazs et al. 2014) (Reprinted with permission, Copyright 2014, American Chemical Society) (**b**) Cilia (black filaments) repel a soft particle (the magenta sphere). The adhesive cilia "heads" are shown as red spheres. The inset shows nodes (in yellow) on a tip, some of which can form sticky bonds with the particle (Balazs et al. 2014). (Reprinted with permission, Copyright 2014, American Chemical Society) (c) Particle sorting by ciliated surfaces based on size: initial state (top image) and final state (bottom) (Tripathi et al. 2013). (Reprinted with permission, Copyright 2013, American Chemical Society). (d) Schematics depicting that cilia can be used to drive away model swimming micro-organisms. The green curved filament indicates the trajectory of the red three-linked-sphere swimmer (Shum et al. 2013) (Reprinted with permission, Copyright 2013, American Chemical Society). (e) Schematics of particle manipulation by passive cilia driven by an oscillating flow induced by horizontally moving the top wall of the channel with a time varying velocity ($U_w(t)$) (Tripathi et al. 2014) (Reprinted with permission, Copyright 2014, American Chemical Society) (color figure online)

surfaces (Zhang et al. 2019). Two types of self-cleaning surfaces were reported: fully ciliated surfaces encompassing orthogonally arranged MAC, and partially ciliated surfaces composed of a central unciliated square region surrounded by 3 rows of MAC on each side. Both types of ciliated surfaces were able to remove microparticles out of the ciliated area due to the generation of substantial flow in combination with direct pushing forces acting on the particles (Fig. 12) (Zhang et al. 2019). Specifically, the fully ciliated surface is capable of removing the vast majority of a large size range (30 to 500 μm) of particles, except for particles that have a diameter close to the cilia pitch and particles that are much smaller than the cilia pitch (Fig. 12d). Moreover, the fully ciliated surface could also repel irregular-shaped sand grains in both water and air. Besides the self-cleaning capability, there is also a possibility to use these ciliated surfaces to sort particles by size since particles of different sizes are repelled along different directions. This was the first proof-of-principle study that showed the promising possibility to harness artificial cilia to create self-cleaning surfaces. Another experimental study demonstrated that MAC can be used to directionally transport a viscoelastic particle in air primarily due to the gravity induced energy transfer from gravitational potential energy to kinetic energy (Ben et al. 2018). Even though the transportation was found to be slow (~90 μm/s), this experimentally proved the feasibility to transport particles with artificial cilia. Moreover, MAC were found to be able to transport water droplets (Kim et al. 2015; Lin et al. 2018; Yang et al. 2018).

Although artificial cilia may offer a promising tool to manipulate particles, more effort needs to be devoted to this topic including miniaturization of artificial cilia, anti-fouling capability studies using real fouling agents, controllability of the particle transporting direction, and cell viability in the case of transporting cells.

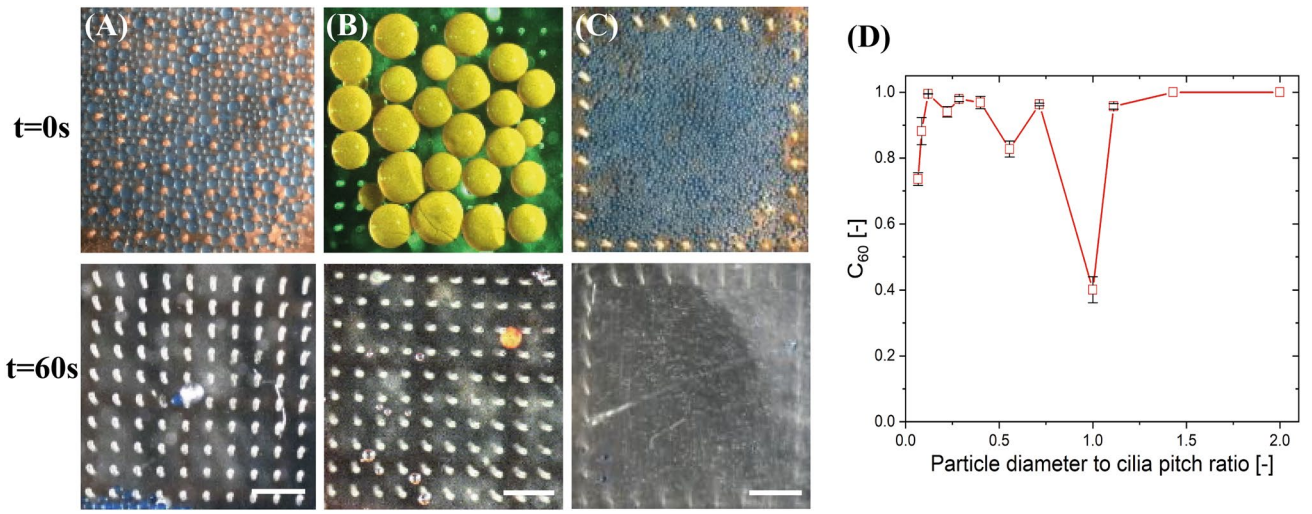

Fig. 12 Particle removal by ciliated surfaces: experiments. Snapshots showing the self-cleaning capability of ciliated surfaces: **a**, **b** A fully ciliated surface of 10 by 10 cilia can remove microparticles of a wide range of sizes, **c** a partially ciliated surface, in which a central region does not have artificial cilia, is also capable of removing microparticles from its central area. The cilia have a diameter of 50 μm, a length of 350 μm and a pitch of 250 μm. All scale bars are 500 μm. **d** Calculated cleaning efficiency as a function of the ratio between the particle diameter and the cilia pitch when the MAC perform a tilted conical motion at 40 Hz for the fully ciliated surface. The cleaning efficiency is defined as $C_{60}=(N_0-N_{60})/N_0$, where N_0 is the number of particles within the ciliated area at the beginning, and N_{60} is the number of particles remaining in the ciliated area after the MAC operating for 60 s. When $C=1$, the ciliated area is completely clean (Zhang et al. 2019) (Reprinted with permission, Copyright 2018, WILEY-VCH Verlag GmbH & Co. KGaA, Weinheim)

5 Conclusions and perspectives

This review covers the major areas of research that targets particle/cell manipulation in a microfluidic environment for applications including bioanalysis, drug delivery, self-cleaning and antifouling. The review includes established methods based on microfluidics, as well as recently proposed innovative methods that still are in the initial phases of development, based on self-propelling microbots and artificial cilia. Rather than going into details for each method, the review offers a broad but still concise overview, explanation, and evaluation of the methods; novel methods based on chemical propulsion and artificial cilia-based manipulation are particularly highlighted. Depending on the specific application, each method has its own advantages and shortcomings that must be balanced against each other depending on the particular application for which it should be used. For example, acoustic tweezers have a wide variety of applications including circulating tumor cell (CTC) isolation (Li et al. 2015), 2D and 3D cell array formation (Shi et al. 2009; Guo et al. 2016), and inter-cellular communication (Guo et al. 2015), but the design of these acoustic tweezers is tedious and the fabrication is costly. Direct magnetic particle manipulation is straightforward, but it requires strong magnetic field gradients so that the effective local working space is small, and it requires biofunctionalized magnetic beads. Notably, different mechanisms can also be combined to achieve better control; for example, hydrodynamic and electrokinetic manipulation can be combined to controllably trap and separate particles in microfluidic devices (Jellema et al. 2009) Self-driven robots are capable of drug delivery without external energy input, at the expense that it can only work in a fuel-containing solvent. Artificial cilia have been demonstrated both numerically and experimentally to be able to manipulate particles and to offer a potential solution to create self-cleaning and antifouling surfaces, but nevertheless, the study of manipulation of particles using artificial cilia is still at the proof-of-principle stage. Table 1 concisely summarizes the operating mechanisms and parameters, applications, resolutions, and system requirements of all the reviewed techniques. Table 2, additionally, shows the primary equation for the force acting on a particle for each manipulation technique, reflecting the dependence on particle properties such as size, density, charge, magnetic susceptibility, and refractive index. These tables combined can be used as an initial guideline for choosing a particle manipulation technique for a specific application.

Other factors must be considered as well. One of those is the maturity of the technique. All microfluidics-based methods are more mature and are being applied in practice. In particular, hydrodynamic methods and magnetic particle manipulation are used in a number of commercial products (Ateya et al. 2008; Puri and Ganguly 2013). The self-driven microbots and the artificial cilia-based methods, on the other hand, are still in early stages of development. Another relevant factor is that, in general, most adopted approaches

Table 1 Summary of operating parameters of particle manipulation techniques

Technique	Mechanism	Main applications	Parameters on which operation is based	Spatial resolution	System requirements
Hydrodynamic methods (Karimi et al. 2013; Bhagat et al. 2008, 2011; Di Carlo et al. 2007; Kuntaegowdanahalli et al. 2009; Wang et al. 2013; Islam et al. 2017; Huang et al. 2004; McGrath et al. 2014; Salafi et al. 2019; Didar and Tabrizian 2010)	Rely on channel shape and structure; the combination of shear forces, inertial effects, and/or boundary effects, results in one or more lateral equilibrium positions of suspended particles, often depending on particle size, shape, deformability or adhesion	Trapping, sorting, enrichment	Size, deformability, shape	> 1 μm	Flow-control devices, multiple pressure regulators, integrated microscopic geometrical features, and/or surface functionalization
Acoustic tweezers (including holographic acoustic tweezers) (Petersson et al. 2004, 2005; Hawkes et al. 2004; Collins et al. 2015; Melde et al. 2016)	Suspended particles gather at either the pressure nodes or the antinodes of acoustic waves under the impact of acoustic radiation forces. Using holography, multiple of such traps can be created dynamically	Sorting, washing, patterning	Size, density, compressibility	> 1 μm	Acoustic sources, Patterned acoustic lens (for holography)
Electrophoresis (Comiskey et al. 1998; Xuan 2019)	Charged particles experience an electrical force, moving the particle within the electrical field depending on charge	Focusing, sorting, trapping, separation	Size, charge, liquid conductivity	> 0.1 μm	Prepatterned electrodes, low-conductivity media
Electro-osmosis (Huang et al. 2010; Xuan 2019; Wu et al. 2016)	Mobile charges in the liquid are set in motion by applying an electric field, creating flow, which transports particles	Focusing, sorting, trapping, separation	Size, liquid conductivity	> 1 μm	Prepatterned electrodes, liquid with mobile charge carriers
Dielectrophoresis (Cummings and Singh 2003; Gadish and Voldman 2006; Adams et al. 2008)	A dielectric particle is subjected to a force in a non-uniform electric field, which moves the particle towards or away from the higher electric field	Sorting, trapping, washing	Size, permittivity	> 0.1 μm	Prepatterned electrodes, low-conductivity media
Optoelectronic tweezers (Wu 2011)	A photosensitive layer is illuminated with light patterns, creating virtual electrodes that induce a local electrical field, resulting in a controlled DEP force	Sorting, trapping, transporting	Size, permittivity	> 0.1 μm	Photosensitive layer, patterned light source, low-conductivity media
Optical tweezers (including holographic optical tweezers) (Arai et al. 1999; MacDonald et al. 2003; Grier and Roichman, 2006)	A laser beam with a Gaussian profile carries momentum that is transferred to the particle; this generates a net force on the particle towards the center of the beam. Using holography, multiple of such traps can be created dynamically	Trapping, separation	Size, refractive index	> 0.1 nm	High-power laser, high-numerical aperture lens, transparent buffers, LC spatial light modulator (for holography)

Table 1 (continued)

Technique	Mechanism	Main applications	Parameters on which operation is based	Spatial resolution	System requirements
Magnetic tweezers (Pamme and Manz 2004; Rida and Gijs 2004; Wang et al. 2011)	In a non-uniform magnetic field, a magnetic or magnetically labelled particle is attracted towards the higher magnetic field	Separation	Size, intrinsic magnetic susceptibility	> 1 μm	Permanent magnet or electromagnets, functionalized magnetic beads
Catalytic reaction powered robots (Paxton et al. 2004; Sen et al. 2008; Sundararajan et al. 2010; Kagan et al. 2010; Mei et al. 2011; Solovev et al. 2009, 2010; Gao et al. 2011, 2012, 2015; Campuzano et al. 2012)	Catalytic reaction generates bubbles at one end of the robot that propel the robot directionally in fuel solutions such as hydrogen peroxide	Pick-up, transport, release	–	~ 1 μm	Fuel solutions
Artificial cilia (Khaderi et al. 2010, 2012; Masoud and Alexeev 2011; Semmler and Alexeev 2011; Dayal et al. 2012; Balazs et al. 2014; Tripathi et al. 2014; Kim et al. 2015; Ben et al. 2018; Lin et al. 2018; Yang et al. 2018; Zhang et al. 2019)	Asymmetric motion of cilia induces local flow, resulting in hydrodynamic forces on the particle. This, in combination with the adhesive forces between the cilia and the particle, enables the cilia to manipulate particles in a controlled manner	Self-cleaning, antifouling, sorting, transport	Size, adhesion strength	~ 30 μm	Actuation setup such as a rotating permanent magnet

Table 2 Equations for the force on a particle for each particle manipulation technique

Technique	Equation/comment	Symbols	References
Hydrodynamic methods	Stokes drag: $F_S = 3\pi\mu a v_p$ Lift force in channel flow: Near the wall: $F_{Lw} = C_L \frac{\rho_L U^2 a^6}{H^4}$ Near the centerline: $F_{Lc} = C_L \frac{\rho_L U^2 a^3}{H^4}$ Dean force: $F_D \sim \rho U^2 a D_h^2 / R_c$	a particle diameter ρ_L liquid density μ liquid viscosity U mean liquid velocity v_p particle velocity C_L lift coefficient H channel height D_h hydraulic diameter R_c radius of curvature of channel	Di Carlo et al. (2007), Karimi et al. (2013)
Acoustic tweezers	Primary radiation force: $F_t = -\left(\frac{\pi p_0^2 V_p \beta_L}{2\lambda}\right) \cdot \phi(\beta, \rho) \cdot \sin(2kx)$ $\phi(\beta, \rho) = \frac{5\rho_p - 2\rho_L}{2\rho_p + \rho_L} - \frac{\beta_p}{\beta_L}$	p_0 acoustic pressure amplitude V_p particle volume β_L liquid compressibility ρ_L liquid density β_p particle compressibility ρ_p particle density λ acoustic wavelength $k = 2\pi/\lambda$ acoustic wave number x distance to pressure node $\phi(\beta, \rho)$ acoustic contrast factor	Laurell et al. (2007)
Electrophoresis	$F_{EP} = ZeE$	Ze charge of particle E electric field magnitude	Bruus (2008)
Electro-osmosis	$F_{EO} \sim \mu a \mu_{EO} E$	a particle diameter μ liquid viscosity μ_{EO} electro-osmotic mobility E electric field magnitude	Bruus (2008)
Dielectrophoresis/optoelectronic tweezers	$F_{DEP} = 2\pi r^3 \mathrm{Re}(f_{CM}) \nabla E_{rms}^2$ $f_{CM} = \frac{\varepsilon_p^* - \varepsilon_L^*}{\varepsilon_p^* + 2\varepsilon_L^*}$	r particle radius E_{rms} rms of the applied electric field f_{CM} Clausius-Mossoti factor ε_p^* complex permittivity of the particle ε_L^* complex permittivity of the liquid	Lenshof and Laurell (2010)
Optical tweezers	Scattering force in direction of wave propagation: $F_{scat} = \frac{I}{c} \frac{128\pi^5 r^6}{3\lambda^4} \left(\frac{N^2-1}{N^2+2}\right)^2 n$ Gradient force towards highest light intensity: $F_{grad} = \frac{-n^3 r^3}{2} \left(\frac{N^2-1}{N^2-2}\right) \nabla I$	r particle radius n refractive index of liquid N ratio of refractive index of particle to index n of medium I light intensity λ wavelength of light c speed of light	Molloy and Padgett (2002)
Magnetic tweezers	$F_{mag} = \frac{V_p \Delta\chi}{\mu_0} (\nabla \cdot B) \cdot B$	V_p particle volume $\Delta\chi$ difference in magnetic susceptibility between particle and fluid μ_0 permeability of vacuum B magnetic flux density	Pamme and Manz (2004)
Catalytic reaction-powered robots	Not described by a specific formula: dependent on catalytic reaction, fuel availability, and geometrical robot design		
Artificial cilia	Not described by a specific formula: dependent on artificial cilia configuration and actuation		

to manipulate particles either need large peripherals, such as electrical control systems or syringe pumps, or they are expensive and/or cumbersome to integrate. Moreover, most of the methods cannot control a single targeted particle among a large population, which is required for some applications such as rare cell investigation in big heterogeneous populations such as CTC analysis. An exception is the use of optical tweezers and, when appropriately adapted,

dielectrophoresis. Last but not least, particle manipulation is mostly just one basic function within a device, and the creation and exploitation of fully integrated portable devices such as point-of-care devices still needs to overcome such challenges as incorporating various assay steps from sample preparation to detection into a single microfluidic chip, the applicability to a diversity of samples and reagents, and ease-of-use.

Even though a vast variety of challenges still need to be tackled, the current research efforts on the manipulation of particles have already led to many promising results and methods, some of which are currently used in practice, and these efforts will in the future further enable compact and portable particle manipulation devices for applications like self-cleaning/antifouling, personalized health care and diagnostics.

Acknowledgements Shuaizhong Zhang was financially supported by the China Scholarship Council.

References

Adams JD, Kim U, Soh HT (2008) Multitarget magnetic activated cell sorter. Proc Natl Acad Sci USA 105:18165–18170. https://doi.org/10.1073/pnas.0809795105

Arai Y, Yasuda R, Akashi K (1999) letters to nature Tying a molecular knot with optical tweezers. Nature 399:446–448

Ashkin A, Dziedzic JM, Chu S (1986) Observation of a single-beam gradient-force optical trap for dielectric particles in air. Opt Lett 22:288–290

Ateya DA, Erickson JS, Howell PB et al (2008) The good, the bad, and the tiny: a review of microflow cytometry. Anal Bioanal Chem 391:1485–1498. https://doi.org/10.1007/s00216-007-1827-5

Balazs AC, Bhattacharya A, Tripathi A, Shum H (2014) Designing bioinspired artificial cilia to regulate particle-surface interactions. J Phys Chem Lett 5:1691–1700. https://doi.org/10.1021/jz5004582

Ben S, Tai J, Ma H et al (2018) Cilia-inspired flexible arrays for intelligent transport of viscoelastic microspheres. Adv Funct Mater 28:1706666. https://doi.org/10.1002/adfm.201706666

Bhagat AAS, Hou HW, Li LD et al (2011) Pinched flow coupled shear-modulated inertial microfluidics for high-throughput rare blood cell separation. Lab Chip 11:1870–1878. https://doi.org/10.1039/c0lc00633e

Bhagat AAS, Kuntaegowdanahalli SS, Papautsky I (2008) Continuous particle separation in spiral microchannels using dean flows and differential migration. Lab Chip 8:1906–1914. https://doi.org/10.1039/b807107a

Bhatia SN, Ingber DE (2014) Microfluidic organs-on-chips. Nat Biotechnol 32:760–772. https://doi.org/10.1038/nbt.2989

Bhattacharya A, Balazs AC (2013) Stiffness-modulated motion of soft microscopic particles over active adhesive cilia. Soft Matter 9:3945–3955. https://doi.org/10.1039/c3sm00028a

Bhattacharya A, Buxton GA, Usta OB, Balazs AC (2012) Propulsion and trapping of microparticles by active cilia arrays. Langmuir 28:3217–3226. https://doi.org/10.1021/la204845v

Blake JR, Sleigh MA (1974) Mechanism of cilia locomotion. Biol Rev 49:85–125

Block SM, Schnitzer MJ (1997) Kinesin hydrolyses one ATP per 8-nm step. Nature 388:386–390

Block SM, Wang MD, Schnitzer MJ et al (1998) Force and velocity measured for single molecules of RNA polymerase. Science (80–) 282:902–907

Bruus H (2008) Theoretical microfluidics. Oxford University Press, Oxford

Callow JA, Callow ME (2011) Trends in the development of environmentally friendly fouling-resistant marine coatings. Nat Commun 2:210–244. https://doi.org/10.1038/ncomms1251

Campuzano S, Orozco J, Kagan D et al (2012) Bacterial isolation by lectin-modified microengines. Nano Lett 12:396–401. https://doi.org/10.1021/nl203717q

Clifford D (1932) Antony van Leeuwenhoek and his "Little animals". Russel & Russel Publishers, New York

Collins DJ, Morahan B, Garcia-Bustos J et al (2015) Two-dimensional single-cell patterning with one cell per well driven by surface acoustic waves. Nat Commun 6:1–11. https://doi.org/10.1038/ncomms9686

Comiskey B, Albert J, Yoshizawa H, Jacobson J (1998) An electrophoretic ink for all-printed reflective electronic displays. Nature 394:253–255

Cummings EB, Singh AK (2003) Dielectrophoresis in microchips containing arrays of insulating posts: Theoretical and experimental results. Anal Chem 75:4724–4731. https://doi.org/10.1021/ac0340612

Darnton N, Turner L, Breuer K, Berg HC (2004) Moving fluid with bacterial carpets. Biophys J 86:1863–1870. https://doi.org/10.1016/S0006-3495(04)74253-8

Dayal P, Kuksenok O, Bhattacharya A, Balazs AC (2012) Chemically-mediated communication in self-oscillating, biomimetic cilia. J Mater Chem 22:241–250. https://doi.org/10.1039/c1jm13787e

den Toonder JMJ, Onck PR (2013a) Artificial cilia. RSC Publishing, Cambridge

den Toonder JMJ, Onck PR (2013b) Microfluidic manipulation with artificial/bioinspired cilia. Trends Biotechnol 31:85–91. https://doi.org/10.1016/j.tibtech.2012.11.005

Dholakia K, Reece P, Gu M (2008) Optical micromanipulation. Chem Soc Rev 37:42–55. https://doi.org/10.1039/b512471a

Di Carlo D, Irimia D, Tompkins RG, Toner M (2007) Continuous inertial focusing, ordering, and separation of particles in microchannels. Proc Natl Acad Sci USA 104:18892–18897. https://doi.org/10.1073/pnas.0704958104

Didar TF, Tabrizian M (2010) Adhesion based detection, sorting and enrichment of cells in microfluidic Lab-on-Chip devices. Lab Chip 10:3043–3053. https://doi.org/10.1039/c0lc00130a

Dittrich PS, Manz A (2006) Lab-on-a-chip: microfluidics in drug discovery. Nat Rev Drug Discov 5:210–218

Enuka Y, Hanukoglu I, Edelheit O et al (2012) Epithelial sodium channels (ENaC) are uniformly distributed on motile cilia in the oviduct and the respiratory airways. Histochem Cell Biol 137:339–353. https://doi.org/10.1007/s00418-011-0904-1

Fauci LJ, Dillon R (2005) Biofluidmechanics of reproduction. Annu Rev Fluid Mech 38:371–394. https://doi.org/10.1146/annurev.fluid.37.061903.175725

Fritz LW, Lutz RA, Foote MA et al (1984) Selective feeding and grazing rates of oyster (*Crassostrea-virginica*) larvae on natural phytoplankton assemblages. Estuaries 7:513–518. https://doi.org/10.2307/1352056

Gadish N, Voldman J (2006) High-throughput positive-dielectrophoretic bioparticle microconcentrator. Anal Chem 78:7870–7876. https://doi.org/10.1021/ac061170i

Gao W, Dong R, Thamphiwatana S et al (2015) Artificial micromotors in the mouse's stomach: a step toward in vivo use of synthetic motors. ACS Nano 9:117–123. https://doi.org/10.1021/nn507097k

Gao W, Sattayasamitsathit S, Orozco J, Wang J (2011) Highly efficient catalytic microengines: template electrosynthesis of polyaniline/platinum microtubes. J Am Chem Soc 133:11862–11864. https://doi.org/10.1021/ja203773g

Gao W, Uygun A, Wang J (2012) Hydrogen-bubble-propelled zinc-based microrockets in strongly acidic media. J Am Chem Soc 134:897–900. https://doi.org/10.1021/ja210874s

Gossett DR, Weaver WM, MacH AJ et al (2010) Label-free cell separation and sorting in microfluidic systems. Anal Bioanal Chem 397:3249–3267. https://doi.org/10.1007/s00216-010-3721-9

Grier DG, Roichman Y (2006) Holographic optical trapping. Appl Opt 45:880–887. https://doi.org/10.1364/AO.45.000880

Guo F, Li P, French JB et al (2015) Controlling cell–cell interactions using surface acoustic waves. Proc Natl Acad Sci USA 112:43–48. https://doi.org/10.1073/pnas.1422068112

Guo F, Mao Z, Chen Y et al (2016) Three-dimensional manipulation of single cells using surface acoustic waves. Proc Natl Acad Sci USA 113:1522–1527. https://doi.org/10.1073/pnas.1524813113

Hawkes JJ, Barber RW, Emerson DR, Coakley WT (2004) Continuous cell washing and mixing driven by an ultrasound standing wave within a microfluidic channel. Lab Chip 4:446–452. https://doi.org/10.1039/b408045a

Hiratsuka Y, Miyata M, Tada T, Uyeda TQP (2006) A microrotary motor powered by bacteria. Proc Natl Acad Sci USA 103:13618–13623. https://doi.org/10.1073/pnas.0604122103

Huang CC, Bazant MZ, Thorsen T (2010) Ultrafast high-pressure AC electro-osmotic pumps for portable biomedical microfluidics. Lab Chip 10:80–85. https://doi.org/10.1039/b915979g

Huang LR, Cox EC, Austin RH, Sturm JC (2004) Continuous particle separation through deterministic lateral displacement. Science (80–) 304:987–990. https://doi.org/10.1126/science.1094567

Islam M, Brink H, Blanche S et al (2017) Microfluidic sorting of cells by viability based on differences in cell stiffness. Sci Rep 7:1–12. https://doi.org/10.1038/s41598-017-01807-z

Jellema LC, Mey T, Koster S, Verpoorte E (2009) Charge-based particle separation in microfluidic devices using combined hydrodynamic and electrokinetic effects. Lab Chip 9:1914–1925. https://doi.org/10.1039/b819054b

Kagan D, Laocharoensuk R, Zimmerman M et al (2010) Rapid delivery of drug carriers propelled and navigated by catalytic nanoshuttles. Small 6:2741–2747. https://doi.org/10.1002/smll.201001257

Kang L, Chung BG, Langer R, Khademhosseini A (2008) Microfluidics for drug discovery and development: from target selection to product lifecycle management. Drug Discov Today 13:1–13. https://doi.org/10.1016/j.drudis.2007.10.003

Karimi A, Yazdi S, Ardekani AM (2013) Hydrodynamic mechanisms of cell and particle trapping in microfluidics. Biomicrofluidics. https://doi.org/10.1063/1.4799787

Khaderi SN, Baltussen MGHM, Anderson PD et al (2010) Breaking of symmetry in microfluidic propulsion driven by artificial cilia. Phys Rev E 82:027302. https://doi.org/10.1103/PhysRevE.82.027302

Khaderi SN, den Toonder JMJ, Onck PR (2012) Fluid flow due to collective non-reciprocal motion of symmetrically-beating artificial cilia. Biomicrofluidics. https://doi.org/10.1063/1.3676068

Kim J, Campbell AS, de Ávila BEF, Wang J (2019) Wearable biosensors for healthcare monitoring. Nat Biotechnol 37:389–406. https://doi.org/10.1038/s41587-019-0045-y

Kim JH, Kang SM, Lee BJ et al (2015) Remote manipulation of droplets on a flexible magnetically responsive film. Sci Rep 5:17843. https://doi.org/10.1038/srep17843

Kim K, Guo J, Liang Z, Fan D (2018) Artificial Micro/nanomachines for bioapplications: biochemical delivery and diagnostic sensing. Adv Funct Mater 28:1–19. https://doi.org/10.1002/adfm.201705867

Kirschner CM, Brennan AB (2012) Bio-inspired antifouling strategies. Annu Rev Mater Res 42:211–229. https://doi.org/10.1146/annurev-matsci-070511-155012

Kitamura K, Tokunaga M, Iwane AH, Yanagida T (2005) A single myosin head moves along an actin filament with regular steps of 5.3 nanometres. Seibutsu Butsuri 40:89–93. https://doi.org/10.2142/biophys.40.89

Kuntaegowdanahalli SS, Bhagat AAS, Kumar G, Papautsky I (2009) Inertial microfluidics for continuous particle separation in spiral microchannels. Lab Chip 9:2973–2980. https://doi.org/10.1039/b908271a

Labarbera M (1984) Feeding currents and particle capture mechanisms in suspension feeding animals. Anim Am Zool 24:71–84. https://doi.org/10.1093/icb/24.1.71

LaBarbera M (1981) Water flow Patterns in and around three species of articulate brachiopods. J Exp Mar Biol Ecol 55:185–206

Laurell T, Petersson F, Nilsson A (2007) Chip integrated strategies for acoustic separation and manipulation of cells and particles. Chem Soc Rev 36:492–506. https://doi.org/10.1039/b601326k

Lenshof A, Laurell T (2010) Continuous separation of cells and particles in microfluidic systems. Chem Soc Rev 39:1203–1217. https://doi.org/10.1039/b915999c

Li P, Mao Z, Peng Z et al (2015) Acoustic separation of circulating tumor cells. Proc Natl Acad Sci USA 112:4970–4975. https://doi.org/10.1073/pnas.1504484112

Lin Y, Hu Z, Zhang M et al (2018) Magnetically induced low adhesive direction of nano/micropillar arrays for microdroplet transport. Adv Funct Mater 28:1800163. https://doi.org/10.1002/adfm.201800163

Lu X, Liu C, Hu G, Xuan X (2017) Particle manipulations in non-Newtonian microfluidics: a review. J Colloid Interface Sci 500:182–201. https://doi.org/10.1016/j.jcis.2017.04.019

MacDonald MP, Spalding GG, Dholakia K (2003) Microfluidic sorting in an optical lattice. Nature 426:421–424. https://doi.org/10.1038/nature02144

Magdanz V, Sanchez S, Schmidt OG (2013) Development of a sperm-flagella driven micro-bio-robot. Adv Mater 25:6581–6588. https://doi.org/10.1002/adma.201302544

Masoud H, Alexeev A (2011) Harnessing synthetic cilia to regulate motion of microparticles. Soft Matter 7:8702–8708. https://doi.org/10.1039/c1sm05423f

McGrath J, Jimenez M, Bridle H (2014) Deterministic lateral displacement for particle separation: a review. Lab Chip 14:4139–4158. https://doi.org/10.1039/c4lc00939h

Mei Y, Solovev AA, Sanchez S, Schmidt OG (2011) Rolled-up nanotech on polymers: from basic perception to self-propelled catalytic microengines. Chem Soc Rev 40:2109–2119. https://doi.org/10.1039/c0cs00078g

Melde K, Mark AG, Qiu T, Fischer P (2016) Holograms for acoustics. Nature 537:518–522. https://doi.org/10.1038/nature19755

Molloy JE, Padgett MJ (2002) Lights, action: optical tweezers. Contemp Phys 43:241–258. https://doi.org/10.1080/00107510110116051

Nguyen NT, Shaegh SAM, Kashaninejad N, Phan DT (2013) Design, fabrication and characterization of drug delivery systems based on lab-on-a-chip technology. Adv Drug Deliv Rev 65:1403–1419. https://doi.org/10.1016/j.addr.2013.05.008

Nguyen NT, Wu Z (2005) Micromixers—a review. J Micromech Microeng 15:1–16. https://doi.org/10.1088/0960-1317/15/2/R01

Nilsson J, Evander M, Hammarström B, Laurell T (2009) Review of cell and particle trapping in microfluidic systems. Anal Chim Acta 649:141–157. https://doi.org/10.1016/j.aca.2009.07.017

Nir S, Reches M (2016) Bio-inspired antifouling approaches: the quest towards non-toxic and non-biocidal materials. Curr Opin Biotechnol 39:48–55. https://doi.org/10.1016/j.copbio.2015.12.012

Nonaka S, Yoshiba S, Watanabe D et al (2005) De novo formation of left-right asymmetry by posterior tilt of nodal cilia. PLoS Biol. https://doi.org/10.1371/journal.pbio.0030268

Ozcelik A, Rufo J, Guo F et al (2018) Acoustic tweezers for the life sciences. Nat Methods 15:1021–1028. https://doi.org/10.1038/s41592-018-0222-9

Pamme N (2007) Continuous flow separations in microfluidic devices. Lab Chip 7:1644–1659. https://doi.org/10.1039/b712784g

Pamme N, Manz A (2004) On-chip free-flow magnetophoresis: continuous flow separation of magnetic particles and agglomerates. Anal Chem 76:7250–7256. https://doi.org/10.1021/ac049183o

Patra D, Sengupta S, Duan W et al (2013) Intelligent, self-powered, drug delivery systems. Nanoscale 5:1273–1283. https://doi.org/10.1039/c2nr32600k

Paxton WF, Kistler KC, Olmeda CC et al (2004) Catalytic nanomotors: Autonomous movement of striped nanorods. J Am Chem Soc 126:13424–13431. https://doi.org/10.1021/ja047697z

Petersson F, Nilsson A, Holm C et al (2004) Separation of lipids from blood utilizing ultrasonic standing waves in microfluidic channels. Analyst 129:938–943. https://doi.org/10.1039/b409139f

Petersson F, Nilsson A, Jönsson H, Laurell T (2005) Carrier medium exchange through ultrasonic particle switching in microfluidic channels. Anal Chem 77:1216–1221. https://doi.org/10.1021/ac048394q

Pohl HA (1951) The motion and precipitation of suspensoids in divergent electric fields. J Appl Phys 22:869–871. https://doi.org/10.1063/1.1700065

Pratt ED, Huang C, Hawkins BG et al (2011) Rare cell capture in microfluidic devices. Chem Eng Sci 66:1508–1522. https://doi.org/10.1016/j.ces.2010.09.012

Puri IK, Ganguly R (2013) Particle transport in therapeutic magnetic fields. Annu Rev Fluid Mech 46:407–440. https://doi.org/10.1146/annurev-fluid-010313-141413

Rida A, Gijs MAM (2004) Manipulation of self-assembled structures of magnetic beads for microfluidic mixing and assaying. Anal Chem 76:6239–6246. https://doi.org/10.1021/ac049415j

Riisgard HU, Larsen PS (2001) Minireview: ciliary filter feeding and bio-fluid mechanics—present understanding and unsolved problems. Limnol Oceanogr 46:882–891

Romero MR, Kelstrup HCP, Strathmann RR (2010) Capture of particles by direct interception by cilia during feeding of a gastropod veliger. Biol Bull 218:145–159. https://doi.org/10.1086/BBLv218n2p145

Ruppert EE, Fox RS, Barnes RD (2004) Invertebrate zoology, 7th edn. Brooks Cole Thomson, Belmont, CA

Sajeesh P, Sen AK (2014) Particle separation and sorting in microfluidic devices: a review. Microfluid Nanofluid 17:1–52. https://doi.org/10.1007/s10404-013-1291-9

Salafi T, Zhang Y, Zhang Y (2019) A review on deterministic lateral displacement for particle separation and detection. Springer, Singapore

Semmler C, Alexeev A (2011) Designing structured surfaces that repel fluid-borne particles. Phys Rev E Stat Nonlinear Soft Matter Phys 84:1–6. https://doi.org/10.1103/PhysRevE.84.066303

Sen A, Sundararajan S, Lammert PE et al (2008) Catalytic motors for transport of colloidal cargo. Nano Lett 8:1271–1276. https://doi.org/10.1021/nl072275j

Shi J, Ahmed D, Mao X et al (2009) Acoustic tweezers: Patterning cells and microparticles using standing surface acoustic waves (SSAW). Lab Chip 9:2890–2895. https://doi.org/10.1039/b910595f

Shum H, Tripathi A, Yeomans JM, Balazs AC (2013) Active ciliated surfaces expel model swimmers. Langmuir 29:12770–12776. https://doi.org/10.1021/la402783x

Sleigh MA (1989) Adaptations of ciliary systems for the propulsion of water and mucus. Comp Biochem Physiol Part A Physiol 94:359–364. https://doi.org/10.1016/0300-9629(89)90559-8

Solovev AA, Mei Y, Ureña EB et al (2009) Catalytic microtubular jet engines self-propelled by accumulated gas bubbles. Small 5:1688–1692. https://doi.org/10.1002/smll.200900021

Solovev AA, Sanchez S, Pumera M et al (2010) Magnetic control of tubular catalytic microbots for the transport, assembly, and delivery of micro-objects. Adv Funct Mater 20:2430–2435. https://doi.org/10.1002/adfm.200902376

Soong RK, Bachand GD, Neves HP et al (2000) Powering an inorganic nanodevice with a biomolecular motor. Science (80–) 290:1555–1558. https://doi.org/10.1126/science.290.5496.1555

Stafford-Smith MG, Ormond RFG (1992) Sediment-rejection mechanisms of 42 species of Australian scleractinian corals. Mar Freshw Res 43:683–705. https://doi.org/10.1071/MF9920683

Strathmann RR, Jahn TL, Fonseca J (1972) Suspension feeding by marine invertebrate larvae: clearance of particles by ciliated bands of a rotifer, pluteus, and trochophore. Biol Bull 142:505–519

Sundararajan S, Sengupta S, Ibele ME, Sen A (2010) Drop-off of colloidal cargo transported by catalytic Pt-Au nanomotors via photochemical stimuli. Small 6:1479–1482. https://doi.org/10.1002/smll.201000227

Taghon GL (1982) Optimal foraging by deposit-feeding invertebrates: roles of particle size and organic coating. Oecologia 52:295–304. https://doi.org/10.1007/BF00367951

Tornay R, Braschler T, Demierre N et al (2008) Dielectrophoresis-based particle exchanger for the manipulation and surface functionalization of particles. Lab Chip 8:267–273. https://doi.org/10.1039/b713776a

Tottori S, Zhang L, Qiu F et al (2012) Magnetic helical micromachines: fabrication, controlled swimming, and cargo transport. Adv Mater 24:811–816. https://doi.org/10.1002/adma.201103818

Tripathi A, Bhattacharya A, Balazs AC (2013) Size selectivity in artificial cilia-particle interactions: mimicking the behavior of suspension feeders. Langmuir 29:4616–4621. https://doi.org/10.1021/la400318f

Tripathi A, Shum H, Balazs AC (2014) Fluid-driven motion of passive cilia enables the layer to expel sticky particles. Soft Matter 10:1416–1427. https://doi.org/10.1039/c3sm52156g

Van Reenen A, De Jong AM, den Toonder JMJ, Prins MWJ (2014) Integrated lab-on-chip biosensing systems based on magnetic particle actuation-a comprehensive review. Lab Chip 14:1966–1986. https://doi.org/10.1039/c3lc51454d

Wahl M, Kröger K, Lenz M (1998) Non-toxic protection against epibiosis. Biofouling 12:205–226. https://doi.org/10.1080/08927019809378355

Wang G, Mao W, Byler R et al (2013) Stiffness dependent separation of cells in a microfluidic device. PLoS ONE. https://doi.org/10.1371/journal.pone.0075901

Wang Y, Dostalek J, Knoll W (2011) Magnetic nanoparticle-enhanced biosensor based on grating-coupled surface plasmon resonance. Anal Chem 83:6202–6207. https://doi.org/10.1021/ac200751s

Whitesides GM (2006) The origins and the future of microfluidics. Nature 442:368–373. https://doi.org/10.1038/nature05058

Wu MC (2011) Optoelectronic tweezers. Nat Photonics 5:322–324. https://doi.org/10.1038/nphoton.2011.98

Wu Y, Ren Y, Tao Y et al (2016) Large-scale single particle and cell trapping based on rotating electric field induced-charge electroosmosis. Anal Chem 88:11791–11798. https://doi.org/10.1021/acs.analchem.6b03413

Xuan X (2019) Recent advances in direct current electrokinetic manipulation of particles for microfluidic applications. Electrophoresis 40:2484–2513. https://doi.org/10.1002/elps.201900048

Xuan X, Zhu J, Church C (2010) Particle focusing in microfluidic devices. Microfluid Nanofluid 9:1–16. https://doi.org/10.1007/s10404-010-0602-7

Yang Z, Park JK, Kim S (2018) Magnetically responsive elastomer–silicon hybrid surfaces for fluid and light manipulation. Small 14:1702839. https://doi.org/10.1002/smll.201702839

Yoshiba S, Shiratori H, Kuo IY et al (2012) Cilia at the node of mouse embryos sense fluid flow for left-right determination via Pkd2. Science (80–) 338:226–231

Yu J, Jin D, Chan KF et al (2019) Active generation and magnetic actuation of microrobotic swarms in bio-fluids. Nat Commun 10:1–12. https://doi.org/10.1038/s41467-019-13576-6

Zhang S, Wang Y, Lavrijsen R et al (2018) Versatile microfluidic flow generated by moulded magnetic artificial cilia. Sensors Actuators B Chem 263:614–624. https://doi.org/10.1016/j.snb.2018.01.189

Zhang S, Wang Y, Onck PR, den Toonder JMJ (2019) Removal of microparticles by ciliated surfaces—an experimental study. Adv Funct Mater 29:1806434. https://doi.org/10.1002/adfm.201806434